Drug Design, Development and Therapy

Dovepress

open access to scientific and medical research

Open Access Full Text Article

ORIGINAL RESEARCH

Knockdown of hsa_circ_0059955 Induces Apoptosis and Cell Cycle Arrest in Nucleus Pulposus Cells via Inhibiting *Itchy E3 Ubiquitin Protein Ligase*

This article was published in the following Dove Press journal:
Drug Design, Development and Therapy

Daliang Kong
Rui Gu
Chengtao Zhang
Ruofeng Yin

Department of Orthopedics, China-Japan Union Hospital, Changchun, Jilin 130031, People's Republic of China

Background: Circular RNAs (circRNAs) play an important role in the progression of intervertebral disc (IVD) degeneration (IVDD). Using bioinformatics analysis, we have found that the expression of circRNA hsa_circ_0059955 was significantly downregulated in IVDD tissues. However, the relevant mechanism of hsa_circ_0059955 in the progression of IVDD remains unclear.

Methods: CCK-8 and flow cytometry assays were used to evaluate cell proliferation and apoptosis. In addition, Western blot assay was used to detect the expressions of ITCH, p73, CDK2 in nucleus pulposus (NP) cells. Moreover, a puncture-induced IVDD rat model was established to explore the role of hsa_circ_0059955 in IVDD.

Results: The level of hsa_circ_0059955 was significantly decreased in IVDD tissues from IVDD patients. *Itchy E3 ubiquitin protein ligase* (ITCH) is the host gene of hsa_circ_0059955, and downregulation of hsa_circ_0059955 significantly decreased the expression of ITCH in NP cells. In addition, downregulation of hsa_circ_0059955 markedly inhibited proliferation and induced apoptosis and cell cycle arrest in NP cells. Moreover, in vivo study illustrated that overexpression of hsa_circ_0059955 ameliorated IVDD in rats.

Conclusion: Downregulation of hsa_circ_0059955 could induce apoptosis and cell cycle arrest in NP cells in vitro, while overexpression of hsa_circ_0059955 attenuated the IVDD in a puncture-induced rat model in vivo. Therefore, hsa_circ_0059955 might serve as a therapeutic target for the treatment of IVDD.

Keywords: intervertebral disc degeneration, hsa_circ_0059955, *Itchy E3 ubiquitin protein ligase*, p73

Introduction

Low back pain (LBP) is one of the most common health problems, influencing the quality of people's life, and leading to huge global economic burden.[1,2] Evidence has been shown that intervertebral disc degeneration (IVDD) is a primary mechanical cause of LBP.[3] In addition, IVDD is characterized by decreased extracellular matrix (ECM), increased cell death and fibrosis.[4] As we know, intervertebral disc is composed of the outer fibrous annulus, cartilaginous endplate and the inner nucleus pulposus (NP).[5] NP is crucial for stabilization of the intervertebral disc.[6] During aging and degeneration of IVDD, senescence and apoptosis were increased in NP.[7,8] Additionally, it has been shown that multiple factors can induce the apoptosis of NP cells including

Correspondence: Ruofeng Yin
Department of Orthopedics, China-Japan Union Hospital, Changchun, Jilin 130031, People's Republic of China
Email yrf_wind@jlu.edu.cn

submit your manuscript | www.dovepress.com
DovePress
http://doi.org/10.2147/DDDT.S253293

infection, genetics, inflammatory cytokines, and signaling networks.[1,9] Recently, cell, growth factor, and gene therapy are the main therapies for the treatment of IVDD;[10] however, current strategies for the treatment of IVDD remains unsatisfying. Therefore, development of effective strategies for the patients with IVDD is extremely required.

Circular RNAs (circRNAs) are another kind of noncoding RNA which form a closed-loop structure without 5′ caps and 3′ tails.[11] Due to the circular structure, circRNAs are highly conserved and stable than linear mRNAs.[12] CircRNAs are mainly located in the cytoplasm,[13] and most of the circRNAs are generated from one or more coding exons via a backsplice mechanism.[11] CircRNAs could promote gene transcription, and function as modifiers of parental gene expression.[14] In addition, many circRNAs involved in several physiological processes including apoptosis, migration, invasion, and tumorigenesis.[15] Moreover, circRNAs are participated in the pathogenesis of many human diseases, such as vascular diseases, cancer, and inflammatory diseases.[16,17] Previous study indicated that circRNAs play an important role in the development and progression of IVDD.[11] However, the role of circRNAs in IVDD has not been fully illuminated.

In the present study, Gene Expression Omnibus (GEO) dataset was performed to identify DEcircRNAs by comparing the expression profiling of circRNAs between IVDD tissues and normal controls. Hsa_circ_0059955 was selected for investigation based on the bioinformatics analysis.

Materials and Methods

Clinical Specimens

Human normal intervertebral discs were obtained from cadaveric donors (9 males and 6 females, the median age of 52, range from 43 to 64) without any spinal disease. Human degenerated intervertebral discs were collected from donors (10 males and 5 females, the median age of 55, range from 47 to 68) undergoing spinal fusion surgery. This study was approved by ethics committees of China-Japan Union Hospital. Written informed consents were obtained by participants or their families.

CircRNA Data Analysis and Bioinformatics

GSE67566 dataset which contains the circRNAs expression data of five IVDD tissues and five normal discs tissues was downloaded from Gene Expression Omnibus (GEO) database (https://www.ncbi.nlm.nih.gov/geo/). The R language was used to screen the DEcircRNAs. CircRNAs exhibiting p-values ≤0.05 and fold changes ≥2.0 were considered evidence of significant difference. Gene ontology (GO, http://www.geneontology.org/) and Kyoto Encyclopedia of Genes and Genomes (KEGG, http://www.genome.jp/kegg/) enrichment analysis was used to conduct the functional analysis and significant pathways of the host genes of circRNAs, as previously described.[18]

Cell Culture

Immortalized human nucleus pulposus cells (NP) cell line was obtained from ScienCell Research Laboratories, Inc. (https://www.sciencellonline.com/human-nucleus-pulposus-cells.html, Carlsbad, CA). Immortalized NP cells are capable of immortalization with maintenance of original NP cell features.[19] Cells were cultured in DMEM medium (Thermo Fisher Scientific, Waltham, MA, USA) supplemented with 10% fetal bovine serum (Thermo Fisher Scientific) and 100 U/mL antibiotics (penicillin and streptomycin) at 37°C in a humidified atmosphere of 5% CO_2. The culture medium was changed every two days.

Lentivirus Production and Stable Cell Lines Construction

Two pairs of cDNA oligonucleotides inhibiting hsa_circ_0059955 expression were inserted into the shRNA expression plasmid (GenePharma, Shanghai, China), named hsa_circ_0059955-shRNA1 and hsa_circ_0059955-shRNA2. Additionally, the hsa_circ_0059955 and ITCH sequences were synthesized by GenePharma (Shanghai) respectively, and then sub-cloned into the lentiviral expression vector. Then, hsa_circ_0059955-shRNA1, hsa_circ_0059955-shRNA2 and, hsa_circ_0059955-overexpression (circRNA-OE), and ITCH-overexpression (ITCH-OE) plasmids were transfected into 293T cells. After 72 h of incubation, the supernatant was collected. NP cells were then infected with hsa_circ_0059955-shRNA1, hsa_circ_0059955-shRNA2, circRNA-OE and ITCH-OE supernatants, respectively, for 24 h. After that, cells were then incubated with puromycin (2.5 μg/mL, Thermo Fisher Scientific) to select stable hsa_circ_0059955 knockdown, hsa_circ_0059955-overexpression or ITCH overexpression cells for another 48 h. The stable cell line was detected by RT-qPCR.

Reverse Transcription-Quantitative Polymerase Chain Reaction (RT-qPCR)

Total RNA was extracted from NP cells by using the TRIzol Regent (Thermo Fisher Scientific) according to the

manufacturer's protocol. M-MLV reverse transcriptase (Takara Bio Inc. Shiga, Japan) was performed to synthesize the cDNA. Real-time PCR analysis was performed using the SYBR Green reagent (Thermo Fisher Scientific) on the ABI Real-Time PCR System (Applied Biosystems, Foster City, CA, USA). The thermocycler programs were as follows: 95°C for 3 min and 40 cycles of 95°C for 10 s, 58°C for 30 s, and 72°C for 30 s. The primer sequences were: Actin: forward, 5′-GTCCACCGCAAATGCTTCTA-3′; reverse, 5′-TGCTGTCACCTTCACCGTTC-3′. Hsa_circ_0059955: forward, 5′-CCATGCCACAGCACATAAAGA-3′; reverse, 5′-GACACCAGAACCGGAAATACTG-3′. The relative level of hsa_circ_0059955 was normalized to β-actin according to the $2^{-\Delta\Delta CT}$ method.[20] β-actin is the calibrator.

Fluorescence in situ Hybridization (FISH) Analysis

Cellular hsa_circ_0059955 expression was detected using FISH with an oligonucleotide probe specific for hsa_circ_0059955. FISH assay was conducted using Ribo™ Fluorescent in situ Hybridization Kit (Ribobio Company, China) as described previously.[21]

Cell Proliferation Assay

NP cells (5 x 10^3 cells/well) were seed onto 96-well plates and incubated overnight at 37°C. Later on, cells were infected with hsa_circ_0059955-shRNA1 for 24, 48 and 72 h, respectively. After that, 10 μL of the Cell Counting kit 8 (CCK-8) reagent (Beyotime, Shanghai, China) was added into each well, and cells were then incubated for another 2 h. The OD value was detected using a microplate reader (Bio-Rad Laboratories, Inc., Hercules, CA, USA) at 450 nm.

Ki67 Immunofluorescence Staining

NP cells (2×10^5) were seeded in six-well plates and incubated overnight at 37°C. Later on, cells were infected with hsa_circ_0059955-shRNA1 for 72 h. Then, cells were fixed by 4% paraformaldehyde, and then incubated with rabbit anti-Ki67 antibody (1:100, Abcam Cambridge, MA, USA) overnight at 4°C. After that, cells were incubated with the horseradish peroxidase-conjugated secondary antibody at room temperature for 1 h, and then stained with 4′,6-diamidino-2-phenylindole (DAPI) for 5 min. Subsequently, cells were observed with a laser confocal microscope (Olympus CX23 Tokyo, Japan). Ki67-positive cells were counted in at least five random fields.

Detection of Mitochondrial Membrane Potentials (MMPs)

NP cells (2×10^5) were seeded in six-well plates and incubated overnight at 37°C. Later on, cells were infected with hsa_circ_0059955-shRNA1 for 72 h. Next, NP cells were washed twice with phosphate-buffered saline (PBS), and then incubated with 1 mL JC-1 staining solution (Thermo Fisher Scientific) in the dark for 25 min at 37°C. After that, stained cells were centrifuged at 2000 rpm × 5 mins, and then washed twice with PBS. Subsequently, cells were resuspended in PBS for analysis by the flow cytometer (FACScan™, BD Biosciences, Franklin Lakes, NJ, USA).

Flow Cytometry Assay

Cell Apoptosis Kit with Annexin V FITC and PI (cat. no. V13242; Thermo Fisher Scientific) was used to assess the cell apoptosis according to the manufacturer's introduction. NP cells (2×10^5) were seeded into six-well plates and then infected with hsa_circ_0059955-shRNA1 for 72 h. After that, cells were harvested and washed with PBS, and then re-suspended in binding buffer. Later on, 2×10^5 cells were stained with 5 μL of propidium iodide (PI) and Annexin V-FITC (Thermo Fisher Scientific) in dark at room temperature for 20 min. Subsequently, the percentage of apoptotic cells was detected with a flow cytometer (BD Biosciences). Signals Annex-V-/IP-, Annexin-V+/PI−, Annexin-V+/PI+, and Annex-V-/IP+ indicated viable, early, late apoptotic and necrotic cells, respectively. The percentage of apoptotic cells was calculated as the (number of apoptotic cells/total number of cells) x 100.

Western Blot Assay

NP cells (2×10^5) were seeded into six-well plates and then infected with hsa_circ_0059955-shRNA1 for 72 h. Total proteins were estimated by bicinchoninic acid assay kit (Beyotime Institute of Biotechnology, China). Then, equal amounts of proteins (30 μg) were loaded on 10% sodium dodecyl sulfate-polyacrylamide gel electrophoresis, and then transferred onto polyvinylidene difluoride (PVDF) membrane (Thermo Fisher Scientific). After that, the membrane was blocked in 5% skimmed milk in trisbuffered saline (TBS) plus 0.1% Tween-20 (TBST) for 1 h at room temperature, and then incubated in primary antibodies at 4°C overnight, including anti-BCL2-Associated X (Bax; 1:1000, Abcam), anti-cleaved caspase 3 (1:1000, Abcam), anti-B-cell lymphoma-2 (Bcl-2; 1:1000, Abcam), anti-cleaved caspase 9 (1:1000, Abcam), anti-β-actin (1:1000, Abcam),

and anti-ITCH (1:1000, Abcam), anti-p73 (1:1000, Abcam), anti-CDK2 (1:1000, Abcam), anti-Cyclin E1 (1:1000, Abcam), anti-c-Myc (1:1000, Abcam), anti-MMP2 (1:1000, Abcam), and aggrecan (1:1000, Abcam). Later on, blots were incubated with the horseradish peroxidase (HRP)-conjugated secondary antibody (Abcam, 1:5000) at room temperature for 1 h. Subsequently, the membrane was visualized using an electrochemiluminescence detection system (Thermo Fisher Scientific). β-actin acted as the internal control. Image J software was used for quantification of protein expression.

Rat IVDD Model

SD rats weighting 225–250 g were obtained from the Animal Center of the Chinese Academy of Sciences (Shanghai, China). Rats were randomly divided into three groups: control group, IVDD model group without treatment, and IVDD model with the treatment of hsa_circ_0059955-shRNA1 lentivirus (IVDD + shRNA1). Animals were kept under standard animal room conditions with a 12 h light/dark cycle and fed a standard laboratory food and water. The experimental protocol was approved by the Animal Care Committee of the China-Japan Union Hospital. Rats were weighed and injected intraperitoneally with 2% (w/v) pentobarbital (40 mg/kg). Then, the surgical procedure was performed as described previously.[22] Briefly, the area between the eighth and ninth coccygeal vertebrae (Co8–Co9) was punctured using a needle of 20-gauge. After surgery, the intervertebral disc was pierced with a needle of 27-gauge, followed by injection of hsa_circ_0059955-shRNA1 lentivirus. The rats were sacrificed at 4 weeks after surgery.

Histopathology Analysis

Rat tail disc tissue (Co7/8) was isolated, decalcified, and then fixed in 4% paraformaldehyde. After that, the sections were embedded in paraffin and then cut into 5 μm sections. Later on, the sections were stained with hematoxylin-eosin (HE) and images were observed with a microscope. The cellularity and morphology of nucleus pulposus and fibrous annulus were examined by another group of experienced histology researchers using a microscope as described previously.[22–24] The histologic score was five for normal disc, 6–11 for moderately degenerated disc, 12–14 for severely degenerated disc.

Measurement of Cytokines by ELISA in vivo

The TNF-α (cat. no. H052) or IL-1β (cat. no. H002) content in serum of the rats was measured with ELISA kits (Nanjing Jiancheng Bioengineering Institute, Jiangsu, China) according to the manufacturer's protocol.

Statistical Analysis

Each group performed at least three independent experiments and all data were expressed as mean ± standard deviation (S.D.). The comparisons among multiple groups were made with one-way analysis of variance (ANOVA) followed by Tukey's tests. $P < 0.05$ was considered to indicate a statistically significant difference.

Results

Identification of DEcircRNAs in IVDD

We analyzed the data GSE67566 from the GEO database containing five IVDD tissues and five normal discs tissues. Hierarchical clustering analysis revealed distinguishable circRNA expression profiles between IVDD tissues and normal discs tissues (Figure 1A). In addition, the average level of each circRNA in both groups was revealed in the scatter plot in Figure 1B. A total of 503 circRNAs were differentially expressed in the IVDD tissues compared to the normal disc tissues, consisting of 281 up-regulated and 222 down-regulated circRNAs. All these DEcircRNAs were displayed in the volcano plot (Figure 1C).

GO Enrichment and KEGG Pathway Analyses

The host genes of DEcircRNAs were analyzed using GO and KEGG analysis. The GO results showed that DEcircRNAs were mainly enriched in "Ubiquitin-like protein transferase activity" and "Ubiquitin-protein transferase activity" (Figure 2A). In addition, KEGG analysis results indicated that DEcircRNAs were mainly enriched in "Ubiquitin mediated proteolysis" (Figure 2B). The data found that 11 DEcircRNAs were associated with ubiquitin mediated proteolysis process. These DEcircRNAs were hsa_circ_0000507, hsa_circ_0018478, hsa_circ_0028190, hsa_circ_0041555, hsa_circ_0043947, hsa_circ_0004789, hsa_circ_0050531, hsa_circ_0003923, hsa_circ_0059955, hsa_circ_0062426, hsa_circ_0006716, and Circular RNA Interactome dataset (https://circinteractome.nia.nih.gov) indicated that the corresponding host genes of these DEcircRNAs were CUL4A, HERC4, ANAPC7, UBE2G1, BRCA1, SMURF2, UBA2, UBE2F, ITCH, PPIL2, UBE2D2 (Figure 2C). Moreover, the relative fold change of circRNAs expression of the eleven genes was compared between IVDD group and normal group using R language. The lowest expression level of hsa_circ_0059955 was observed in IVDD tissues (Figure 2D). RT-qPCR results indicated that the level of

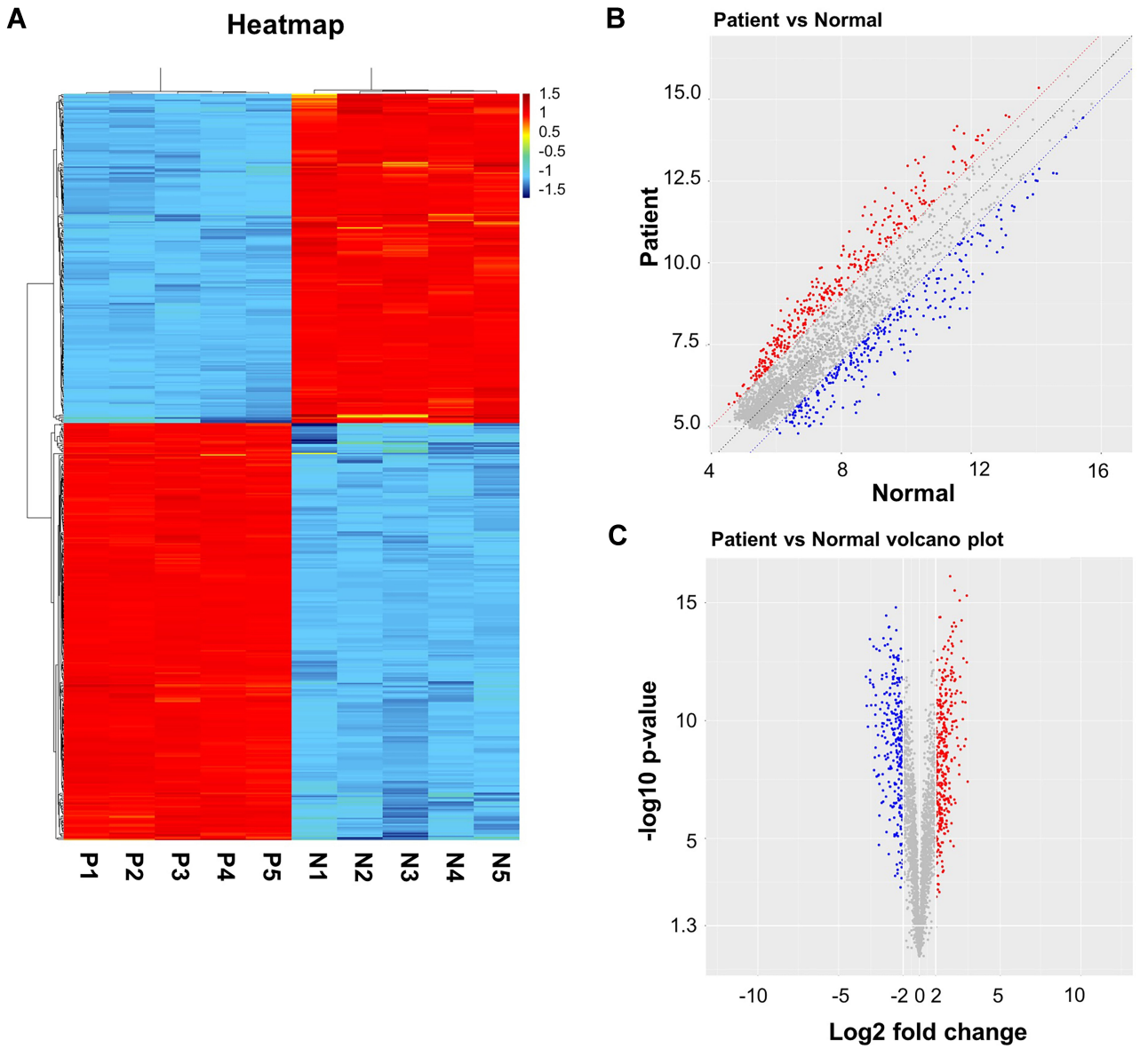

Figure 1 CircRNAs are differentially expressed in IVDD tissues and normal controls. (**A**) Hierarchical clustering heat map showing the circRNA expression profiles of IVDD tissues (P group) and normal controls (N group) according to P value, which downloaded from GSE67566 dataset. (**B**) Scatter plot revealed the normalized circRNA expression in patient group and normal group. The y-axis represented the circRNA level in patient group. The x-axis represented the circRNA level in normal group. (**C**) Volcano plot of DEcircRNAs in GSE67566. The red spots represented high-expressed circRNAs, and the blue spots represented low-expressed circRNAs. P-value <0.05 (-log10 p-value > 1.3) and |log2 Fold Change| > 2 were set as the threshold.

hsa_circ_0059955 was significantly downregulated in the IVDD tissues from patients compared to the normal disc tissues (Figure 2E). Thus, hsa_circ_0059955 was selected for the subsequent experiments.

Downregulation of hsa_circ_0059955 Inhibited Proliferation of NP Cells

To validate the existence of hsa_circ_0059955 in NP cells, FISH assay was performed. As shown in Figure 3A, hsa_circ_0059955 was found to be mainly distributed in the cytoplasm of NP cells. Next, to investigate the role of hsa_circ_0059955 in NP cells, we used two shRNAs (hsa_circ_0059955 shRNA1, hsa_circ_0059955 shRNA2) to downregulate hsa_circ_0059955 in NP cells. As shown in Figure 3B, hsa_circ_0059955 shRNA1 downregulated hsa_circ_0059955 more significantly than hsa_circ_0059955 shRNA2 in NP cells. Thus, hsa_circ_0059955-shRNA1 was utilized in the following experiments. In addition, CCK-8 and Ki67 immunofluorescence assays indicated that down-regulation of hsa_circ_0059955 markedly inhibited

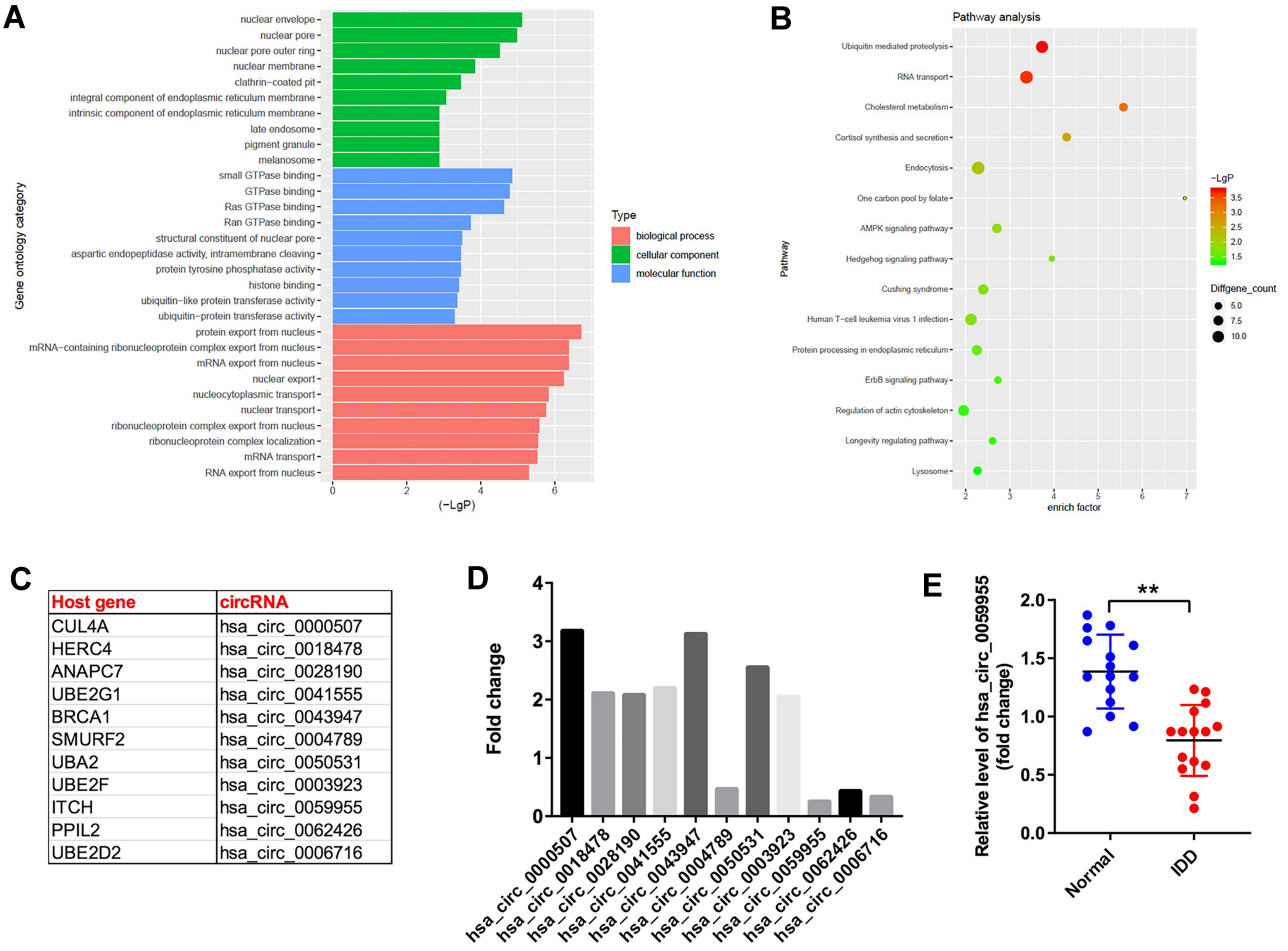

Host gene	circRNA
CUL4A	hsa_circ_0000507
HERC4	hsa_circ_0018478
ANAPC7	hsa_circ_0028190
UBE2G1	hsa_circ_0041555
BRCA1	hsa_circ_0043947
SMURF2	hsa_circ_0004789
UBA2	hsa_circ_0050531
UBE2F	hsa_circ_0003923
ITCH	hsa_circ_0059955
PPIL2	hsa_circ_0062426
UBE2D2	hsa_circ_0006716

Figure 2 GO enrichment and KEGG pathway analyses. (**A**) Overlapping DEcircRNAs were measured by GO enrichment analysis. (**B**) Overlapping DEcircRNAs were measured by KEGG pathway analysis. (**C**) The top 11 DEcircRNAs was identified using R language. DEcircRNAs' host genes were obtained from online bioinformatics analysis tool circular RNA interactome. (**D**) 11 dysregulated circRNAs from IVDD tissues and normal controls were identified using R language. (**E**) The level of hsa_circ_0059955 in the IVDD tissues from patients and in normal disc tissues from cadaveric donors was detected using qRT-PCR. **P < 0.01, compared with the normal group.

proliferation of NP cells (Figure 3C-E). These data suggested that downregulation of hsa_circ_0059955 could inhibit the proliferation of NP cells.

Downregulation of hsa_circ_0059955 Induced Apoptosis of NP Cells

To further explore whether hsa_circ_0059955 knockdown could affect mitochondrial function in NP cells, JC-1 staining assay was performed. As indicated in Figure 4A, silencing of hsa_circ_0059955 significantly decreased the MMP in NP cells (Figure 4A). In addition, downregulation of hsa_circ_0059955 notably induced apoptosis of NP cells, compared with the blank group (Figure 4B and C). Moreover, downregulation of hsa_circ_0059955 markedly increased the expressions of Bax, cleaved caspase 3 and cleaved caspase 9, and notably decreased the expression of Bcl-2 in NP cells (Figure 4D-H). All these results indicated that hsa_circ_0059955 knockdown could induce apoptosis of NP cells.

Downregulation of hsa_circ_0059955 Induced G0/G1 Phase Arrest in NP Cells

Evidence has been shown that circRNAs can regulate the progression of human cancers through regulating transcription of their host genes.[25] However, the regulatory role of hsa_circ_0059955 in the expression of ITCH in NP cells remains unclear. Thus, Western blot assay was used to detect the expression of ITCH in hsa_circ_0059955-knockdown NP cells. As indicated in Figure 5A and B, downregulation of hsa_circ_0059955 notably decreased the level of ITCH in NP cells. In addition, hsa_circ_0059955 knockdown significantly downregulated the levels of CDK2, Cyclin E1 and

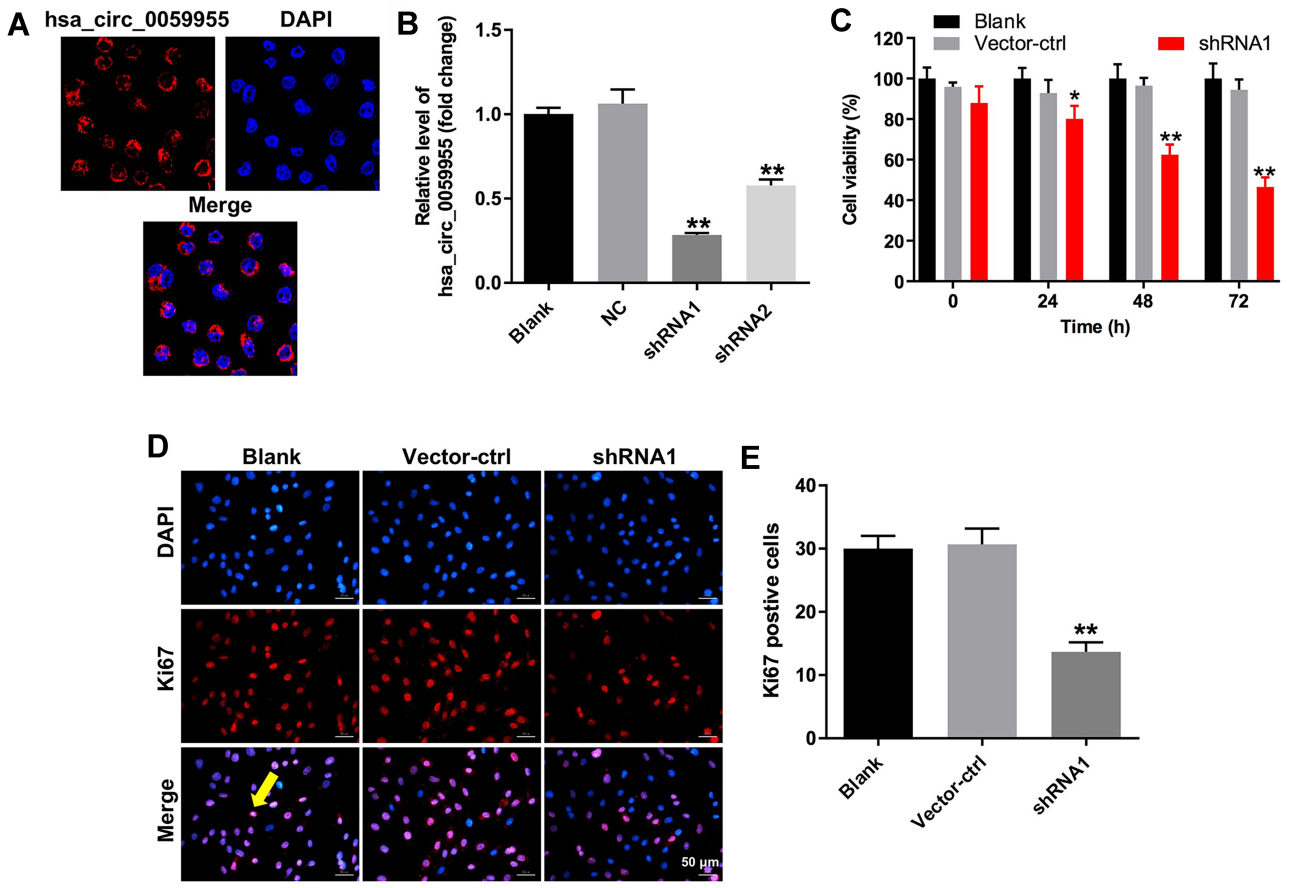

Figure 3 Downregulation of hsa_circ_0059955 inhibited proliferation of NP cells. (**A**) The cellular localization of hsa_circ_0059955 in NP cells was analyzed using FISH assay. (**B**) The level of hsa_circ_0059955 in NP cells infected with hsa_circ_0059955-shRNA1 or hsa_circ_0059955-shRNA2 was detected using qRT-PCR. The experiment was repeated triply. (**C**) NP cells were infected with hsa_circ_0059955-shRNA1 for 0, 24, 48 and 72 h. CCK-8 assay was applied to determine the cell viability, and the experiment was performed in quintuplicate. (**D, E**) NP cells were infected with hsa_circ_0059955-shRNA1 for 72 h. Representative immunofluorescence images showing ki67 (in red), DAPI (in blue) and the merged panel with ki67 and DAPI in NP cells. Arrow in the merged panel indicates a ki67-positive cell (pink color) in NP cells. Scale bar, 50 μm. The experiment was repeated triply. **P < 0.01, compared with the blank group.

c-Myc, and upregulated the level of p73 in NP cells (5A, 5C, 5D, 5E and 5F). In addition, cell cycle distribution of NP cells in each group was assessed using flow cytometry. The data indicated that cells in the G0-G1 stage of the hsa_circ_0059955-shRNA1 group were increased, while cells in the S stage were relatively decreased, compare with vector-ctrl group (Figure 5G and H). These data suggested that downregulation of hsa_circ_0059955 could induce G0/G1 phase arrest in NP cells.

Downregulation of hsa_circ_0059955 Inhibited Proliferation of NP Cells via Inhibition of ITCH

We further investigated whether hsa_circ_0059955 knockdown could inhibit the proliferation of NP cells by downregulating the expression of ITCH. As shown in Figure 6A and B, the expression of ITCH was significantly upregulated in NP cells after transfected with ITCH-OE plasmids. CCK-8 and Ki67 immunofluorescence assays indicated that knockdown of hsa_circ_0059955 markedly suppressed proliferation of NP cells; however, these changes were reversed by ITCH overexpression (Figure 6C-E). These data indicated that downregulation of hsa_circ_0059955 could inhibit proliferation of NP cells via inhibition of ITCH.

Overexpression of hsa_circ_0059955 Ameliorated IVDD of Rats in vivo

To explore the role of hsa_circ_0059955 in rat IVDD model, hsa_circ_0059955-OE lentivirus was injected into the rat intervertebral disc to overexpress hsa_circ_0059955 after IVDD surgery. As shown in Figure 7A, NP cells gradually reduced and were replaced by fibrous tissue and the orderly arrangement of fibrous annulus was fractured and destroyed in the IVDD group. However,

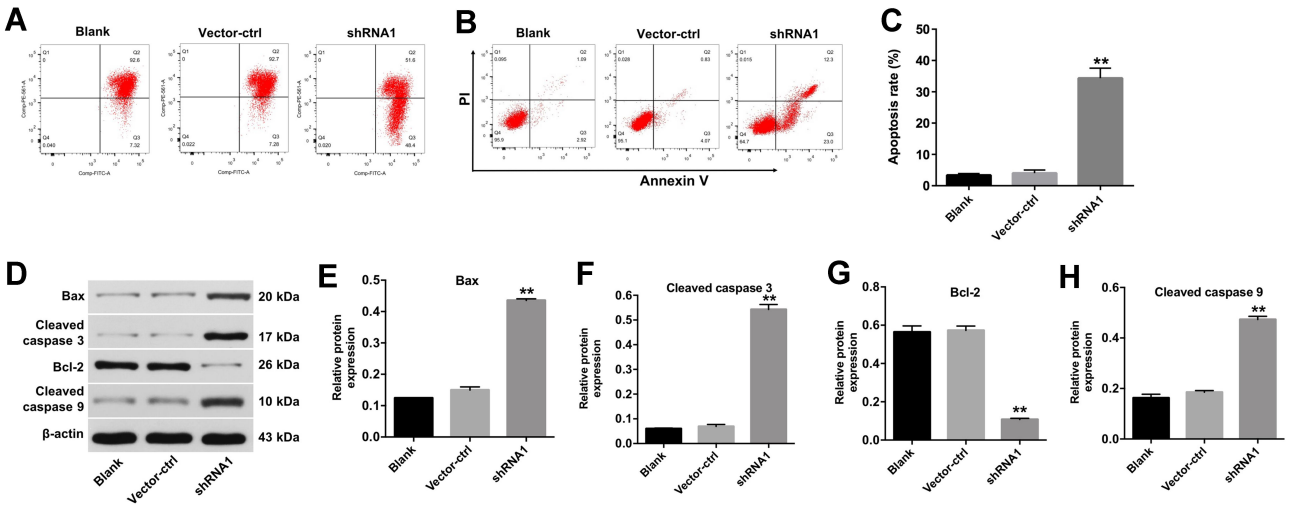

Figure 4 Downregulation of hsa_circ_0059955 induced apoptosis of NP cells. NP cells were infected with hsa_circ_0059955-shRNA1 for 72 h. (**A**) Changes in MMP evaluated via JC-1 staining and flow cytometry. (**B**) Apoptotic cells were detected with Annexin V and PI double staining. (**C**) The apoptotic cell rates were calculated. (**D**) Expressions of Bax, cleaved caspase 3, Bcl-2 and cleaved caspase 9 in NP cells were detected with Western blotting. (**E–H**) The relative expressions of Bax, cleaved caspase 3, Bcl-2 and cleaved caspase 9 in NP cells were quantified via normalization to β-actin. These experiments were repeated triply. **P < 0.01, compared with the blank group.

overexpression of hsa_circ_0059955 obviously alleviated the destruction of disc structure compared with the IVDD group (Figure 7A). In addition, the histologic score of the IVDD + circRNA-OE group was significantly lower than that of the IVDD group (Figure 7B). Moreover, the levels of TNF-α and IL-1β were significantly increased in the serum of a rat IVDD model, compared with those of the control group; however, these changes were reversed by hsa_circ_0059955 OE (Figure 7C and D). Meanwhile, the expression of matrix metalloproteinases 2 (MMP2) was notably upregulated and the level of aggrecan was significantly decreased in the degenerated disc compared with those of the control group; however, these changes were reversed by hsa_circ_0059955 OE (Figure 7E-G). All these data indicated that overexpression of hsa_circ_0059955 could ameliorate IVDD in rats in vivo.

Discussion

CircRNAs are ubiquitously expressed in human tissues, including human intervertebral disc tissue.[26] However, the specific function of most circRNAs in IVDD remains largely unclear. Using bioinformatics analysis, we have identified 503 DEcircRNAs between IVDD tissues and normal discs tissues using R language. KEGG analysis results indicated that DEcircRNAs were mainly enriched in ubiquitin mediated proteolysis process. Jin et al indicated that ubiquitin pathways participated in cell proliferation and cell apoptosis in the progression of IVDD.[27] From the above analysis, 11 DEcircRNAs were identified including 7 upregulated circRNAs and 4 downregulated circRNAs, which were associated with ubiquitin mediated proteolysis process. The lowest expression level of hsa_circ_0059955 was observed in IVDD tissues. Thus, hsa_circ_0059955 was selected for the subsequent experiments.

IVDD is characterized by decreased cell proliferation and increased cell death.[28] In this study, downregulation of hsa_circ_0059955 significantly inhibited proliferation, and induced apoptosis of NP cells. These data indicated that decreased expression of hsa_circ_0059955 may contribute to IVDD progression. In addition, mitochondrial dysfunction is closely related to the development and progression of IVDD.[29] Moreover, mitochondrial-mediated cell apoptosis generally participated in the progression of IVDD.[30] The mitochondrial apoptosis pathway is induced mainly by apoptotic signals.[31] Apoptotic signals could lead to the loss of MMP, and cause the release of cytochrome c from the mitochondria into the cytosol.[31,32] Bcl-2 family proteins could maintain the mitochondrial integrity, including pro-apoptotic protein Bax, and anti-apoptotic protein Bcl-2.[33] Bax could trigger the release of cytochrome c into the cytosol via regulation of the mitochondrial permeability.[34] After that, cytochrome c recruits caspase-9 to form the apoptosome, and then induces caspase-3 activation and induces apoptosis.[35] In this study, downregulation of hsa_circ_0059955 decreased the MMP in NP cells. Meanwhile, downregulation of hsa_circ_0059955 downregulated the level of Bcl-2, and upregulated the expressions of Bax, cleaved caspase 9 and cleaved caspase 3 in NP cells.

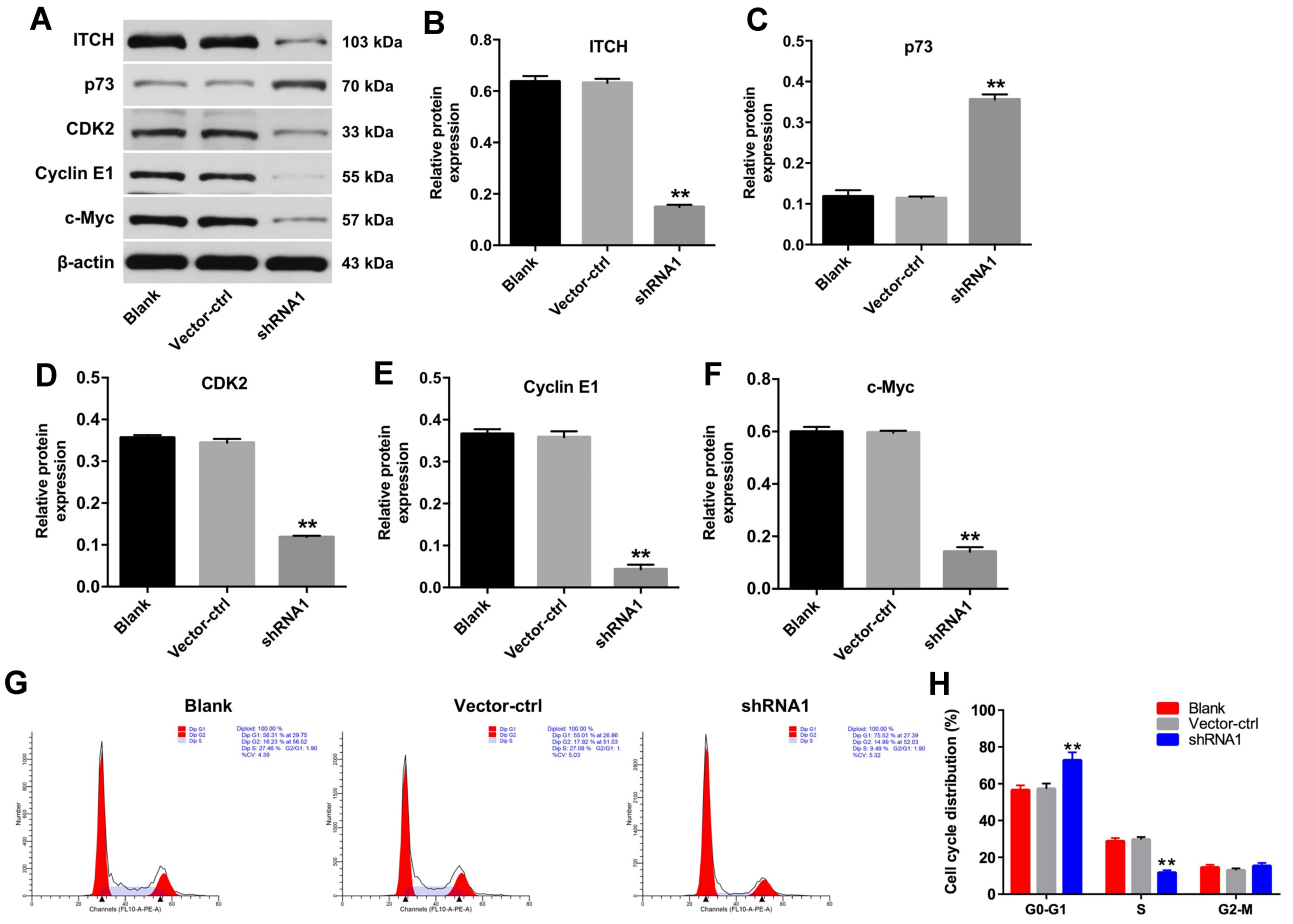

Figure 5 Downregulation of hsa_circ_0059955 induced G0/G1 phase arrest in NP cells. NP cells were infected with hsa_circ_0059955-shRNA1 for 72 h. (**A**) Expressions of ITCH, p73, CDK2, Cyclin E1 and c-Myc in NP cells were detected with Western blotting. (**B–F**) The relative expressions of ITCH, p73, CDK2, Cyclin E1 and c-Myc in NP cells were quantified via normalization to β-actin. (**G, H**) Cell cycle distribution was detected with PI staining. These experiments were repeated triply. **P < 0.01, compared with the blank group.

Ding et al indicated that compression could induce the apoptosis of NP cells via decreasing the MMP and downregulation of Bax.[36] These data indicated that downregulation of hsa_circ_0059955 could induce apoptosis of NP cells via the mitochondrial apoptotic pathway.

Inflammation response plays vital roles in the initiation and exacerbation of IVDD.[37] Evidence has been shown that IL-1β and TNF-α levels are highly expressed in degenerative IVD tissues.[38] In this study, we found that the levels of TNF-α and IL-1β were significantly increased in the serum of a rat IVDD model; however, these changes were reversed by hsa_circ_0059955 overexpression. Moreover, increased levels of IL-1β and TNF-α in NP can induce an imbalance between anabolic and catabolic activities of NPs, including increased expression of catabolic factors (eg, MMPs) and decreased generation of anabolic factors (eg, aggrecan).[11] In this study, we found that the level of MMP2 was increased, while the expression of aggrecan was decreased in the degenerated disc in a puncture-induced rat model; however, these changes were reversed by hsa_circ_0059955 overexpression. These data suggested that overexpression of hsa_circ_0059955 could alleviate inflammatory response, and recover the balance between anabolic and catabolic processes within the NP microenvironment.

Circular RNA interactome (https://circinteractome.nia.nih.gov) revealed that the host gene of hsa_circ_0059955 is ITCH. Ubiquitylation could regulate protein substrates via posttranslational protein modifications.[39] ITCH, a kind of ubiquitin ligases, could promote the ubiquitylation and degradation of p73.[40] The protein p73 is a homologue of p53, which could induce cell apoptosis and cell cycle arrest.[41] Meanwhile, upregulation of p73 could increase the proportion of cells in G1 stage, and decrease the proportion of cells in S stage, indicating that p73 could induce G1 arrest.[41] In this study, downregulation of hsa_circ_0059955 significantly reduced the expression of ITCH, and increased

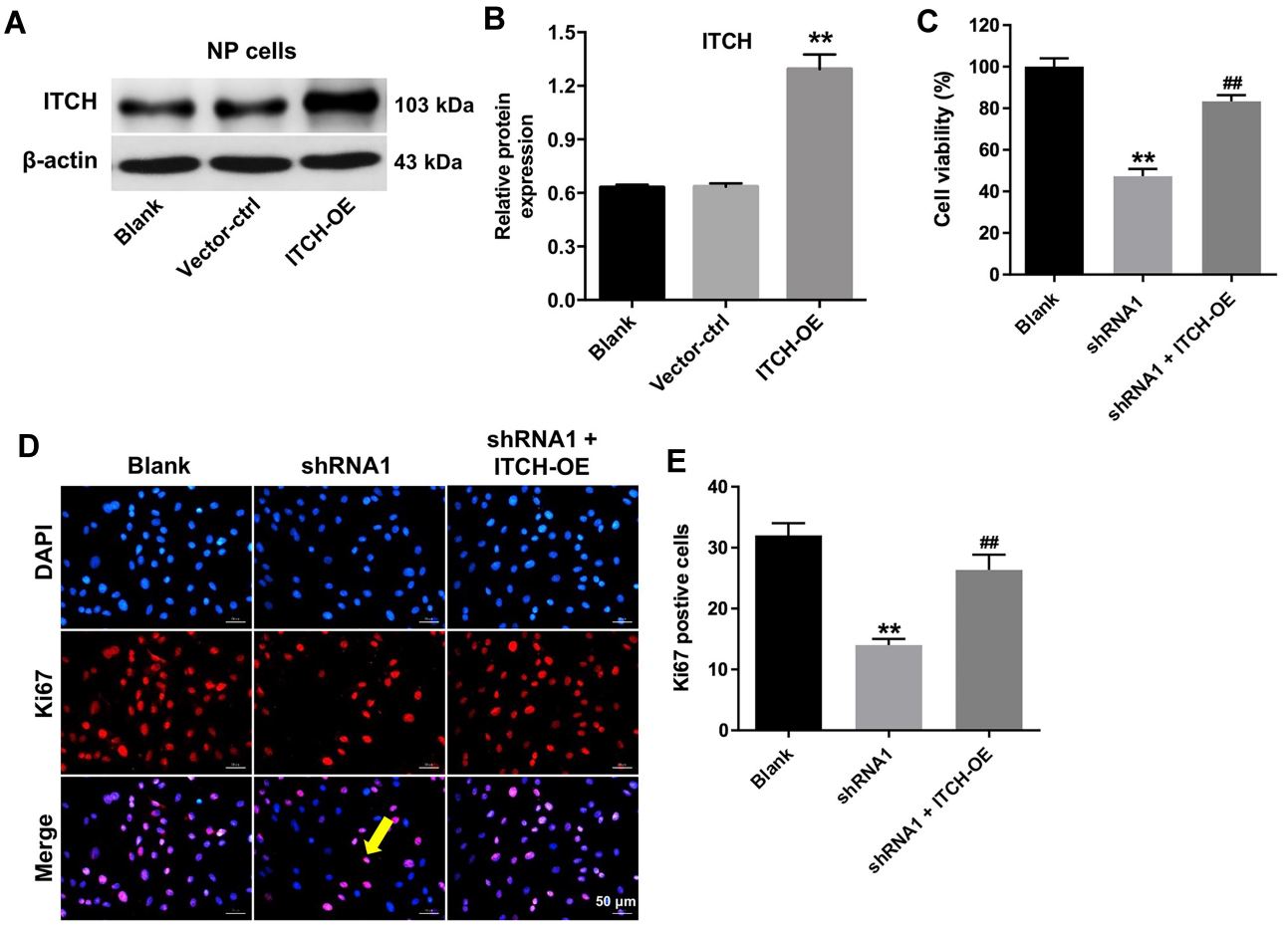

Figure 6 Downregulation of hsa_circ_0059955 inhibited the growth of NP cells via inhibition of ITCH. (**A, B**) The level of ITCH in NP cells infected with ITCH-OE was detected using Western blot. (**C**) NP cells were infected with hsa_circ_0059955-shRNA1 or hsa_circ_0059955-shRNA1 plus ITCH-OE for 72 h. CCK-8 assay was applied to determine the cell viability. (**D, E**) Representative immunofluorescence images showing ki67 (in red), DAPI (in blue) and the merged panel with ki67 and DAPI in NP cells. Arrow in the merged panel indicates a ki67-positive cell (pink color) in NP cells. Scale bar, 50 μm. These experiments were repeated triply. **P < 0.01, compared with the blank group. ##P < 0.01, compared with the shRNA1 group.

the level of p73 in NP cells. In addition, downregulation of hsa_circ_0059955 induced G0/G1 phase arrest in NP cells via downregulation the levels of CDK2, cyclin E1 and c-Myc. These data indicated that downregulation of ITCH in NP cells reduced ITCH-mediated p73 ubiquitylation, and inhibited p73 degradation. The release of p73 induced cell cycle arrest and then triggered apoptosis in NP cells. Previous study indicated that protoporphyrin IX could induce the apoptosis in TP53-deficient cancer cells via inhibition of p73 degradation by ubiquitin ligase ITCH, which was consistent with our results.[42] Collectively, downregulation of hsa_circ_0059955 inhibited the growth of NP cells via downregulation of ITCH, and then inhibition of the degradation p73, finally inducing cell cycle arrest.

Song et al found that circularRNA_104670 could regulate the progression of IVDD via a ceRNA-mediated mechanism, in which circularRNA_104670 functions as an endogenous miR-17-3p sponge.[43] Unlike the classical ceRNA mechanism, zhou et al found that circRNA-ENO1 could promote tumor growth and metastasis in lung adenocarcinoma via regulating its host gene ENO1.[44] In addition, Li et al found that circITGA7 could inhibit growth and metastasis in colorectal cancer cells through upregulating transcription of its host gene ITGA7.[25] According to the data in the circular RNA interactome dataset, hsa_circ_0059955 may interact with multiple proteins. In this study, we found that hsa_circ_0059955 could regulate the expression of its host gene, ITCH, via affecting gene transcription; however, further studies are needed to verify this hypothesis. In addition, our data indicated that hsa_circ_0059955 level was significantly downregulated in the IVDD tissues from patients; however, the correlation between the expression of hsa_circ_0059955 and disc degeneration grade remains unclear. Therefore, further studies are needed to clarify whether the expression of hsa_circ_0059955

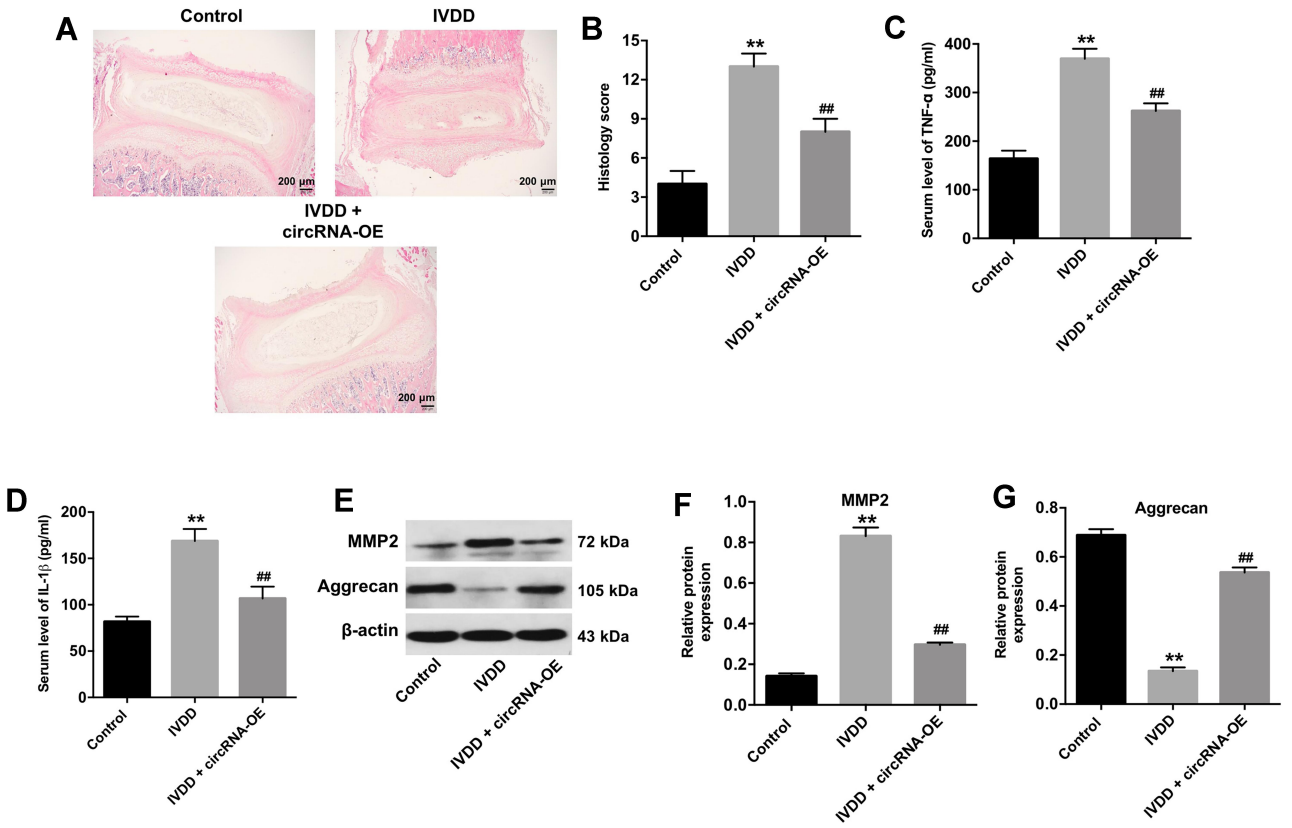

Figure 7 Overexpression of hsa_circ_0059955 ameliorated IVDD in rats in vivo. (**A**) Representative HE staining of NP tissues and fibrous annulus tissues. Scale bar, 200 μm. (**B**) The histological grades of control, IVDD and IVDD + shRNA1 groups. (**C, D**) ELISA assay was applied to detect the levels of TNF-α and IL-1β in the serum of rats. (**E–G**) Expressions of MMP2 and aggrecan in the disc were detected with Western blotting. The relative expressions of MMP2 and aggrecan were quantified via normalization to β-actin. **P < 0.01, compared with the blank group; ##P < 0.01, compared with the IVDD group.

is correlated with disc degeneration grade. Moreover, our data indicated that overexpression of ITCH in NP cells reversed the anti-proliferation effect of hsa_circ_0059955 knockdown, indicating that ITCH might promote proliferation of NP cells. However, the exact role and regulatory mechanism of ITCH in IVDD should be further explored.

Conclusion

In summary, downregulation of hsa_circ_0059955 induced apoptosis and cell cycle arrest in NP cells via inhibition of ITCH. Therefore, hsa_circ_0059955 might be a therapeutic target for the treatment of IVDD.

Disclosure

The authors report no conflicts of interest for this work.

References

1. Long J, Wang X, Du X, et al. JAG2/Notch2 inhibits intervertebral disc degeneration by modulating cell proliferation, apoptosis, and extracellular matrix. *Arthritis Res Ther*. 2019;21(1):213. doi:10.1186/s13075-019-1990-z
2. Jiang C, Guo Q, Jin Y, et al. Inhibition of EZH2 ameliorates cartilage endplate degeneration and attenuates the progression of intervertebral disc degeneration via demethylation of Sox-9. *EBioMedicine*. 2019;48:619–629. doi:10.1016/j.ebiom.2019.10.006
3. Vergroesen PP, Kingma I, Emanuel KS, et al. Mechanics and biology in intervertebral disc degeneration: a vicious circle. *Osteoarthritis Cartilage*. 2015;23(7):1057–1070. doi:10.1016/j.joca.2015.03.028
4. Wang SZ, Rui YF, Lu J, Wang C. Cell and molecular biology of intervertebral disc degeneration: current understanding and implications for potential therapeutic strategies. *Cell Prolif*. 2014;47(5):381–390. doi:10.1111/cpr.12121
5. Sowa G, Vadala G, Studer R, et al. Characterization of intervertebral disc aging: longitudinal analysis of a rabbit model by magnetic resonance imaging, histology, and gene expression. *Spine (Phila Pa 1976)*. 2008;33(17):1821–1828. doi:10.1097/BRS.0b013e31817e2ce3
6. Chen J, Xie JJ, Jin MY, et al. Sirt6 overexpression suppresses senescence and apoptosis of nucleus pulposus cells by inducing autophagy in a model of intervertebral disc degeneration. *Cell Death Dis*. 2018;9(2):56. doi:10.1038/s41419-017-0085-5
7. Zhao CQ, Wang LM, Jiang LS, Dai LY. The cell biology of intervertebral disc aging and degeneration. *Ageing Res Rev*. 2007;6(3):247–261. doi:10.1016/j.arr.2007.08.001
8. Jiang L, Zhang X, Zheng X, et al. Apoptosis, senescence, and autophagy in rat nucleus pulposus cells: implications for diabetic intervertebral disc degeneration. *J Orthop Res*. 2013;31(5):692–702. doi:10.1002/jor.22289

9. Hadjipavlou AG, Tzermiadianos MN, Bogduk N, Zindrick MR. The pathophysiology of disc degeneration: a critical review. *J Bone Joint Surg Br*. 2008;90(10):1261–1270. doi:10.1302/0301-620X.90B10.20910
10. Sampara P, Banala RR, Vemuri SK, Av GR, Gpv S. Understanding the molecular biology of intervertebral disc degeneration and potential gene therapy strategies for regeneration: a review. *Gene Ther*. 2018;25(2):67–82. doi:10.1038/s41434-018-0004-0
11. Cheng X, Zhang L, Zhang K, et al. Circular RNA VMA21 protects against intervertebral disc degeneration through targeting miR-200c and X linked inhibitor-of-apoptosis protein. *Ann Rheum Dis*. 2018;77(5):770–779. doi:10.1136/annrheumdis-2017-212056
12. Li J, Yang J, Zhou P, et al. Circular RNAs in cancer: novel insights into origins, properties, functions and implications. *Am J Cancer Res*. 2015;5(2):472–480.
13. Zhou S, Jiang H, Li M, et al. Circular RNA hsa_circ_0016070 is associated with pulmonary arterial hypertension by promoting PASMC proliferation. *Mol Ther Nucleic Acids*. 2019;18:275–284. doi:10.1016/j.omtn.2019.08.026
14. Qu S, Yang X, Li X, et al. Circular RNA: a new star of noncoding RNAs. *Cancer Lett*. 2015;365(2):141–148. doi:10.1016/j.canlet.2015.06.003
15. Meng S, Zhou H, Feng Z, et al. CircRNA: functions and properties of a novel potential biomarker for cancer. *Mol Cancer*. 2017;16(1):94. doi:10.1186/s12943-017-0663-2
16. Ding S, Zhu Y, Liang Y, et al. Circular RNAs in vascular functions and diseases. *Adv Exp Med Biol*. 2018;1087:287–297.
17. Ye YL, Yin J, Hu T, et al. Increased circulating circular RNA_103516 is a novel biomarker for inflammatory bowel disease in adult patients. *World J Gastroenterol*. 2019;25(41):6273–6288. doi:10.3748/wjg.v25.i41.6273
18. Weng Y, Wu J, Li L, et al. Circular RNA expression profile in the spinal cord of morphine tolerated rats and screen of putative key circRNAs. *Mol Brain*. 2019;12(1):79. doi:10.1186/s13041-019-0498-4
19. Sakai D, Mochida J, Yamamoto Y, et al. Immortalization of human nucleus pulposus cells by a recombinant SV40 adenovirus vector: establishment of a novel cell line for the study of human nucleus pulposus cells. *Spine (Phila Pa 1976)*. 2004;29(14):1515–1523. doi:10.1097/01.BRS.0000131419.25265.23
20. Livak KJ, Schmittgen TD. Analysis of relative gene expression data using real-time quantitative PCR and the 2(-Delta Delta C(T)) method. *Methods*. 2001;25(4):402–408. doi:10.1006/meth.2001.1262
21. Zhan Y, Chen Z, Li Y, et al. Long non-coding RNA DANCR promotes malignant phenotypes of bladder cancer cells by modulating the miR-149/MSI2 axis as a ceRNA. *J Exp Clin Cancer Res*. 2018;37(1):273. doi:10.1186/s13046-018-0921-1
22. Chen D, Xia D, Pan Z, et al. Metformin protects against apoptosis and senescence in nucleus pulposus cells and ameliorates disc degeneration in vivo. *Cell Death Dis*. 2016;7(10):e2441. doi:10.1038/cddis.2016.334
23. Han B, Zhu K, Li FC, et al. A simple disc degeneration model induced by percutaneous needle puncture in the rat tail. *Spine (Phila Pa 1976)*. 2008;33(18):1925–1934. doi:10.1097/BRS.0b013e31817c64a9
24. Mao HJ, Chen QX, Han B, et al. The effect of injection volume on disc degeneration in a rat tail model. *Spine (Phila Pa 1976)*. 2011;36(16):E1062–1069. doi:10.1097/BRS.0b013e3182027d42
25. Li X, Wang J, Zhang C, et al. Circular RNA circITGA7 inhibits colorectal cancer growth and metastasis by modulating the Ras pathway and upregulating transcription of its host gene ITGA7. *J Pathol*. 2018;246(2):166–179. doi:10.1002/path.5125
26. Zou F, Ding Z, Jiang J, et al. Confirmation and preliminary analysis of circRNAs potentially involved in human intervertebral disc degeneration. *Mol Med Rep*. 2017;16(6):9173–9180. doi:10.3892/mmr.2017.7718
27. Jin LZ, Lu JS, Gao JW. Silencing SUMO2 promotes protection against degradation and apoptosis of nucleus pulposus cells through p53 signaling pathway in intervertebral disc degeneration. *Biosci Rep*. 2018;38:3. doi:10.1042/BSR20171523
28. Wang W, Wang J, Zhang J, Taq W, Zhang Z. miR222 induces apoptosis in human intervertebral disc nucleus pulposus cells by targeting Bcl2. *Mol Med Rep*. 2019;20(6):4875–4882. doi:10.3892/mmr.2019.10732
29. Zhang B, Xu L, Zhuo N, Shen J. Resveratrol protects against mitochondrial dysfunction through autophagy activation in human nucleus pulposus cells. *Biochem Biophys Res Commun*. 2017;493(1):373–381. doi:10.1016/j.bbrc.2017.09.015
30. Rannou F, Lee TS, Zhou RH, et al. Intervertebral disc degeneration: the role of the mitochondrial pathway in annulus fibrosus cell apoptosis induced by overload. *Am J Pathol*. 2004;164(3):915–924. doi:10.1016/S0002-9440(10)63179-3
31. Xu X, Wang D, Zheng C, et al. Progerin accumulation in nucleus pulposus cells impairs mitochondrial function and induces intervertebral disc degeneration and therapeutic effects of sulforaphane. *Theranostics*. 2019;9(8):2252–2267. doi:10.7150/thno.30658
32. Hu Y, Shao Z, Cai X, et al. Mitochondrial pathway is involved in advanced glycation end products-induced apoptosis of rabbit annulus fibrosus cells. *Spine (Phila Pa 1976)*. 2019;44(10):E585–e595. doi:10.1097/BRS.0000000000002930
33. Zhang J, Niu H, Zhao ZJ, et al. CRISPR/Cas9 knockout of bak mediates bax translocation to mitochondria in response to TNFalpha/CHX-induced apoptosis. *Biomed Res Int*. 2019;2019:9071297. doi:10.1155/2019/9071297
34. Petit E, Cartron PF, Oliver L, Vallette FM. The phosphorylation of Metaxin 1 controls Bak activation during TNFalpha induced cell death. *Cell Signal*. 2017;30:171–178. doi:10.1016/j.cellsig.2016.11.008
35. Zhang F, Zhao X, Shen H, Zhang C. Molecular mechanisms of cell death in intervertebral disc degeneration (Review). *Int J Mol Med*. 2016;37(6):1439–1448. doi:10.3892/ijmm.2016.2573
36. Ding F, Shao ZW, Yang SH, et al. Role of mitochondrial pathway in compression-induced apoptosis of nucleus pulposus cells. *Apoptosis*. 2012;17(6):579–590. doi:10.1007/s10495-012-0708-3
37. Zhang Y, He F, Chen Z, et al. Melatonin modulates IL-1β-induced extracellular matrix remodeling in human nucleus pulposus cells and attenuates rat intervertebral disc degeneration and inflammation. *Aging (Albany NY)*. 2019;11(22):10499–10512. doi:10.18632/aging.102472
38. Séguin CA, Bojarski M, Pilliar RM, Roughley PJ, Kandel RA. Differential regulation of matrix degrading enzymes in a TNFalpha-induced model of nucleus pulposus tissue degeneration. *Matrix Biol*. 2006;25(7):409–418. doi:10.1016/j.matbio.2006.07.002
39. Hershko A. The ubiquitin system for protein degradation and some of its roles in the control of the cell division cycle. *Cell Death Differ*. 2005;12(9):1191–1197. doi:10.1038/sj.cdd.4401702
40. Rossi M, Rotblat B, Ansell K, et al. High throughput screening for inhibitors of the HECT ubiquitin E3 ligase ITCH identifies antidepressant drugs as regulators of autophagy. *Cell Death Dis*. 2014;5:e1203. doi:10.1038/cddis.2014.113
41. Wu H, Leng RP. MDM2 mediates p73 ubiquitination: a new molecular mechanism for suppression of p73 function. *Oncotarget*. 2015;6(25):21479–21492. doi:10.18632/oncotarget.4086
42. Sznarkowska A, Kostecka A, Kawiak A, et al. Array. *Cell Div*. 2018;13:10. doi:10.1186/s13008-018-0043-3
43. Song J, Wang HL, Song KH, et al. CircularRNA_104670 plays a critical role in intervertebral disc degeneration by functioning as a ceRNA. *Exp Mol Med*. 2018;50(8):94. doi:10.1038/s12276-018-0125-y
44. Zhou J, Zhang S, Chen Z, et al. CircRNA-ENO1 promoted glycolysis and tumor progression in lung adenocarcinoma through upregulating its host gene ENO1. *Cell Death Dis*. 2019;10(12):885. doi:10.1038/s41419-019-2127-7